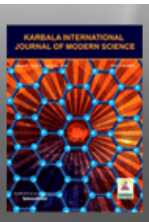

Karbala International Journal of Modern Science

Volume 8 | Issue 1 Article 12

Development of Effectual Substrates for SERS by Nanostructurs-Coated Porous Silicon

Fatima J. Moaen
University of Baghdad College of Sciences, Iraq, fatimaalgaese@yahoo.com

Hammad R. Humud
University of Baghdad College of Sciences, Iraq

Fouad G. Hamzah
Iraqi Ministry of Education, Iraq

Recommended Citation

Moaen, Fatima J.; Humud, Hammad R.; and Hamzah, Fouad G. (2022) "Development of Effectual Substrates for SERS by Nanostructurs-Coated Porous Silicon," *Karbala International Journal of Modern Science*: Vol. 8 : Iss. 1 , Article 12.
Available at: https://doi.org/10.33640/2405-609X.3203

Development of Effectual Substrates for SERS by Nanostructurs-Coated Porous Silicon

Abstract

The current paper provides an efficient method for making active and effectual substrates used for detecting molecules by improving surface-enhanced Raman scattering (SERS). These substrates were fabricated using nanostructure-coated porous silicon. The nanostructures were prepared through the electrical exploding wire (EEW) technique. The silver nanowires (AgNWs) were coated with a polydopamine (PDA) layer to form an AgNWs@PDA colloidal solution. Then, the Ag wire was electrically exploded in the colloidal solution to form the (AgNWs@PDA@AgNPs) plasmonic nanostructures as a metal-insulator-metal. The effect of the plasmonic nanostructures' morphologies on the absorptances spectra and SERS activities were studied utilising Rhodamine 6G (Rh6G) dye as examination molecules. X-ray diffraction (XRD) was used to investigate the structural properties of these nanostructures. Field-emission scanning electron microscopy (FE-SEM) and transmission electron microscopy (TEM) were used to investigate the morphologies of these nanostructures. Atomic force microscopy (AFM) was used to study the surface topographies of SERS-effectual substrates. A double beam UV-Visible Spectrophotometer was used to measure Rh6G laser dye absorptance with a concentration of M) that mixed with the nanostructures at different concentrations. Sunshine Raman spectrometer with a (50 x) objective lens was used to analyse the Raman spectra of Rh6G Sunshine Raman spectrometer with a (50 x) objective lens was used to analyse the Raman spectra of Rh6G dye using a porous silicon substrate (PSi) on which silver nanowires are deposited (PSi-AgNWs). Another porous silicon substrate (PSi) on which nanostructures are deposited that consisting of silver nanowires, coated with a polydopamine layer, and decorated with silver nanoparticles are deposited (PSi-AgNWs@PDA@AgNPs). The results showed that hot spots and roughness on the nanostructures' surfaces caused an increase in intensities of absorptances spectra and signals of SERS. After the effectual substrates were excited by a ($\lambda_{exc.}$=532nm) laser source, the enhancement factor (EF) of SERS signals of Rh6G (1 M) attained (26.3) and (28.7) of the characteristic peaks at wavenumber (1650) for PSi-AgNWs and PSi-AgNWs@PDA@AgNPs effectual substrates respectively. This study showed that nanostructure-coated porous silicon substrates have a repeatable and high signal frequency, stability in storage, cost-low technique, and ease of use. They allow researchers to recognise and analyse a wide range of molecules, including biomolecules, with detection limits ranging between milli- and femtomolar. These effectual substrates have a bright future as a bioanalytical tool using SERS spectroscopy.

Keywords

Surface-enhanced Raman scattering (SERS), electric exploding wire (EEW), porous silicon, plasmonic nanostructure, detection limit

RESEARCH PAPER

Development of Effectual Substrates for SERS by Nanostructure-Coated Porous Silicon

Fatima J. Moaen [a,*], Hammad R. Humud [a], Fouad G. Hamzah [b]

[a] University of Baghdad College of Sciences, Iraq
[b] Iraqi Ministry of Education, Iraq

Abstract

The current paper provides an efficient method for making active and effectual substrates used for detecting molecules by improving surface-enhanced Raman scattering (SERS). These substrates were fabricated using nanostructure-coated porous silicon. The nanostructures were prepared through the electrical exploding wire (EEW) technique. The silver nanowires (AgNWs) were coated with a polydopamine (PDA) layer to form an AgNWs@PDA colloidal solution. Then, the Ag wire was electrically exploded in the colloidal solution to form the (AgNWs@PDA@AgNPs) plasmonic nanostructures as a metal-insulator-metal. The effect of the plasmonic nanostructures' morphologies on the absorptances spectra and SERS activities were studied utilising Rhodamine 6G (Rh6G) dye as examination molecules. X-ray diffraction (XRD) was used to investigate the structural properties of these nanostructures. Field-emission scanning electron microscopy (FE-SEM) and transmission electron microscopy (TEM) were used to investigate the morphologies of these nanostructures. Atomic force microscopy (AFM) was used to study the surface topographies of SERS-effectual substrates. A double beam UV-Visible Spectrophotometer was used to measure Rh6G laser dye absorptance with a concentration of 1×10^{-6} M) that mixed with the nanostructures at different concentrations. Sunshine Raman spectrometer with a (50 x) objective lens was used to analyse the Raman spectra of Rh6G Sunshine Raman spectrometer with a (50 x) objective lens was used to analyse the Raman spectra of Rh6G dye using a porous silicon substrate (PSi) on which silver nanowires are deposited (PSi-AgNWs). Another porous silicon substrate (PSi) on which nanostructures are deposited that consisting of silver nanowires, coated with a polydopamine layer, and decorated with silver nanoparticles are deposited (PSi-AgNWs@PDA@AgNPs). The results showed that hot spots and roughness on the nanostructures' surfaces caused an increase in intensities of absorptances spectra and signals of SERS. After the effectual substrates were excited by a ($\lambda_{exc.} = 532$ nm) laser source, the enhancement factor (EF) of SERS signals of Rh6G (1×10^{-6} M) attained (26.3×10^5) and (28.7×10^5) of the characteristic peaks at wavenumber (1650 cm^{-1}) for PSi-AgNWs and PSi-AgNWs@PDA@AgNPs effectual substrates respectively. This study showed that nanostructure-coated porous silicon substrates have a repeatable and high signal frequency, stability in storage, cost-low technique, and ease of use. They allow researchers to recognise and analyse a wide range of molecules, including biomolecules, with detection limits ranging between milli- and femtomolar. These effectual substrates have a bright future as a bioanalytical tool using SERS spectroscopy.

Keywords: Surface-enhanced Raman scattering (SERS), Electric exploding wire (EEW), Porous silicon, Plasmonic nanostructure, Detection limit

1. Introduction

Surface Plasmon polaritons (SPPs) are the oscillations of electrons at metal-dielectric interfaces when excited by electromagnetic (EM) radiation. SPPs are usually formed at the surface of noble metals. SPPs find widespread use in optical and biological fields and data storage. The confinement of SPPs in nano sits stands for the localised-surface Plasmon resonance (LSPR) [1]. The interaction of

Received 11 July 2021; revised 5 December 2021; accepted 6 December 2021.
Available online 23 February 2022.

* Corresponding author at:
E-mail addresses: fatimaalgaese@yahoo.com (F.J. Moaen), dr.hammad6000@yahoo.com (H.R. Humud), fghhamzah@gmail.com (F.G. Hamzah).

https://doi.org/10.33640/2405-609X.3203

analyte molecules with the SERS substrate, which is usually a surface-roughened or nanostructured metal, is critical to the technique's operation [2]. In addition to greatly increasing Raman emission, SERS interactions may differ from those in a bulk Raman sample. SERS prove their flexibility through the following properties: they (a) combine the inherent properties of Raman identification abilities due to the vibrational fingerprints of the molecules; (b) involve a non-destructive analysis technique; (c) require a smallest amount of prepared sample; and (d) can carry out certain tests with their inherent advantages [3]. In certain situations, it might also be possible to detect a single molecule. Biosensors, analytical chemistry, medical diagnostics and theragnostic have all been proposed as applications for SERS [4,5].

The massive Raman enhancement can usually be explained by two well-known mechanisms, electromagnetic (EM) mechanism and chemical (CM) mechanism. The EM mechanism estimates the degree of the electric field magnified due to the LSPR phenomenon associated with the plasmonic nanostructure. The charge transfer mechanism between non-chemisorbed and chemisorbed species and the substrate mater is revealed by the CM mechanism [3,6,7]. SERS substrates are often engineered to maximise hotspot density by using their enhancement performance to the fullest [8,9]. Effectual substrates of SERS have largely been influenced by plasmonic noble metals (e.g., Au, Ag) and metal nanostructures with rough surfaces. The metal nanostructures supply the substrate with plasmonic coupling via "hot spots" to improve the Raman signal through an EM mechanism [5,10]. The most widely used SERS substrates are silver (Ag) nanostructures. Ag nanostructures of various morphologies, such as nanorods, nanowires, nanospheres and nanosheets, have been chosen as effectual substrates of SERS that allow for detecting little concentration of molecules [11,12].

According to the EM mechanism, to improve the Raman signal, it was necessary to manufacture nanostructures that have a large set of hot spots in addition to its surface roughness. These nanostructures are used as effectual substrates in the SERS technique. As a result, nanostructures having a sufficient abundance of hot spots were designed and manufactured to increase the SERS signal and detect molecules (e.g., Rh6G dye molecules) at exceptionally low concentrations [6,10]. The effect of hot spots is well understood to be dependent on the shape and size of nanoparticles as well as the distance between two adjacent nanoparticles. Theoretical computations have shown that the spacer of adjacent nanoparticles on every surface can supply a significant improvement. The presence of gaps up to the nano-scale between two metals in the nanostructures also helps achieve a noticeable upgrade in the SERS signal [13].

Porous silicon (PSi) is a sponge-like network of crystalline silicon pillars and nodules with nanometre-sized pillars and nodules. Material surface properties serve as the most important aspect in delicate chemical analytics sensing. The ability to differentiate detection tools and their contents are influenced by factors such as surface area, porosity, topography, morphology, and surface functionality [14]. In addition to attractive properties like being environmentally friendly, convenient, functional, and cost-effective, PSi has different physical properties depending on its shape, pore diameter, porosity, and porous thickness. PSi is divided into three types of groups based on the pore width: the nano, meso and macro-PSi [5,14]. PSi is fabricated by the anodic electrochemical etching technique of monocrystalline Si in HF-based electrolytes. The presence of HF molecules is necessary and required for Si etching (coming from the electrolyte) and holes (coming from the silicon wafer) in the reaction interface. To produce enough holes and electrons in the Si, its surface must therefore be exposed to radiation in the anodising process [15].

Dopamine (DA) can be used as a multipurpose rostrum due to its abundant amine and catechol effectual groups on its surface as well as other distinguishing properties such as anchor strength, chemical recognition, and self-polymerisation [12]. Immersing the material in the solution produces the self-polymerisation of dopamine (PDA). PDA may provide a convenient and active procedure for modifying the surface and the development of an extremely strong adherent layer. The PDA molecules display strong complexing behaviours with metallic ions. These behaviours can be lessened in locations unique to metallic nanoparticles through oxidisation of catechol into the equivalent quinine groups via an alkaline aqueous mixture due to abundant, influential groups on the surface such as amine and catechol [16,17].

The EEW process proves to be one of the most promising methods for producing large metal nanoparticles as well as metal and multi-metallic nanostructures [18,19]. As a result, coarse metal nanostructures of proper size and coating are deposited on a variety of surfaces to form effectual substrates. This includes extremely hydrophobic surfaces, providing a potential opportunity to construct sharpened edges and nano-gaps on the silver nanowires (AgNWs) surface as reusable SERS

"hot spots." The silver nanoparticles (AgNPs) were adorned on the surface of the PDA layer using the EEW process to construct (metal-insulator-metal) nanostructures. These nanostructures allow the electric fields generated by AgNPs' LSPR to overlap [6,18].

2. Materials and method

The Rhodamine 6G (Rh6G) dye, whose molecular formula is $C_{28}H_{31}N_2O_3Cl$ and molecular weight 479.01 g/mol, was obtained from Merck Sigma-Aldrich CO. Bearing a weight of 0.047901 g as a powder, it was mixed with 1 mL deionised water to obtain a solution of the Rh6G dye with an initial concentration of 1×10^{-1} M. Then, this concentration was diluted to obtain different concentrations ranging from 1×10^{-6} M to 1×10^{-14} M. An aqueous colloidal of AgNWs, 500 mg dissolved in 25 mL water, with a length of 1 μm and average diameter of 90 nm was obtained from XFNANO. The concentration of aqueous colloidal was ≈0.2 M. Silver wire at 99.9% purity with a diameter of 0.3 mm and silver plate dimensions of 3 cm × 2 cm × 3 mm were obtained from jewellers in Baghdad, Iraq. Dopamine hydrochloride with Tris-base (≥99.9%) was obtained from Merck KGaA. ATOMIC ABSORPTANC SPECTROPHOTOMETER SHIMADZU (AA-7000) was used to measure concentration. X-ray diffraction (XRD) was used to analyse the specifics of internal nanostructure features. A few drops of AgNWs, AgNWs@PDA and AgNWs@PDA@AgNPs nanostructures were dried on a glass substrate. XRD data was taken of 2θ ranged from 10° to 80°. The XRD samples were examined by an X-ray Diffractometer device using a Radiation: CuKα_1 λ: 1.54056 Å from Jonson Matthy Company, Ltd. CAS. Silicon wafers with orientation (100), n-type and thickness of 508–15 μm were used. PSi is made using the electrochemical etching (ECE) process. The morphological and structural properties of the PSi layer and the SERS-effectual substrate were studied using the FE-SEM techniques. The surface morphology of the PSi was examined using the TT-2 AFM workshop. Using a SHIMADZU-1800 UV-Visible double beam spectrophotometer, the absorptances spectra of the mixed Rh6G dye with prepared nanostructures were analysed at room temperature for all samples for different concentrations in the wavelength from 300 nm to 800 nm. After dropping a few drops of Rh6G dye with different concentrations on the effectual substrates and letting them dry under normal conditions, Raman spectra were examined for the various concentrations. Raman spectra of these samples were examined using a Sunshine Raman spectrometer system and after they were excited by a laser source with a wavelength of 532 nm, where the objective lens (50×). The laser power was 4.2 mW and the integration time was 2s.

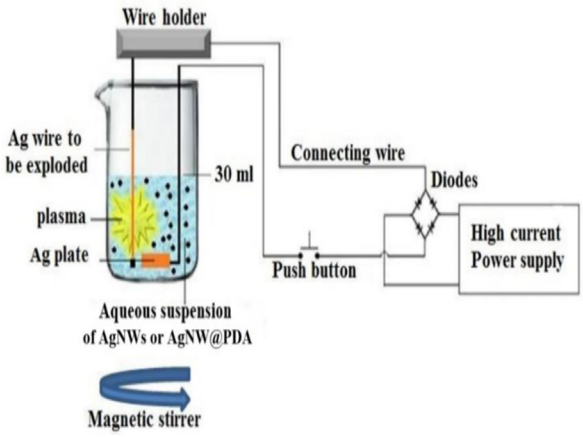

Fig. 1. Experimental set-up for fabricating the AgNWs@PDA@AgNPs nanostructures [18].

2.1. Preparation of (AgNWs@PDA@AgNPs) nanostructures

1.25 mL of silver nanowire (i.e., AgNWs) colloidal with 0.2 M was scattered in 60 mL of deionised water with magnetic stirring for 30 minutes at room temperature. Then, the solution was ultra-sonicated for 15 minutes to ensure full dispersion before adding 0.05 g of dopamine hydrochloride powder. An aqueous colloidal was then preserved in deionised water to be used later. The PDA-coated AgNWs was ultrasonically scattered in 30 mL of deionised water. Silver nanoparticles decorated the surface of AgNWs@PDA by an EEW process to create the AgNWs@PDA@AgNPs nanostructures as shown in Fig. 1.

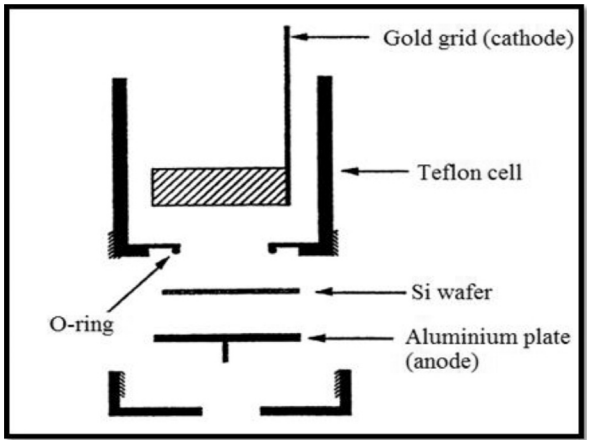

Fig. 2. Electrochemical etching system to fabricate porous silicon (PSi) [14].

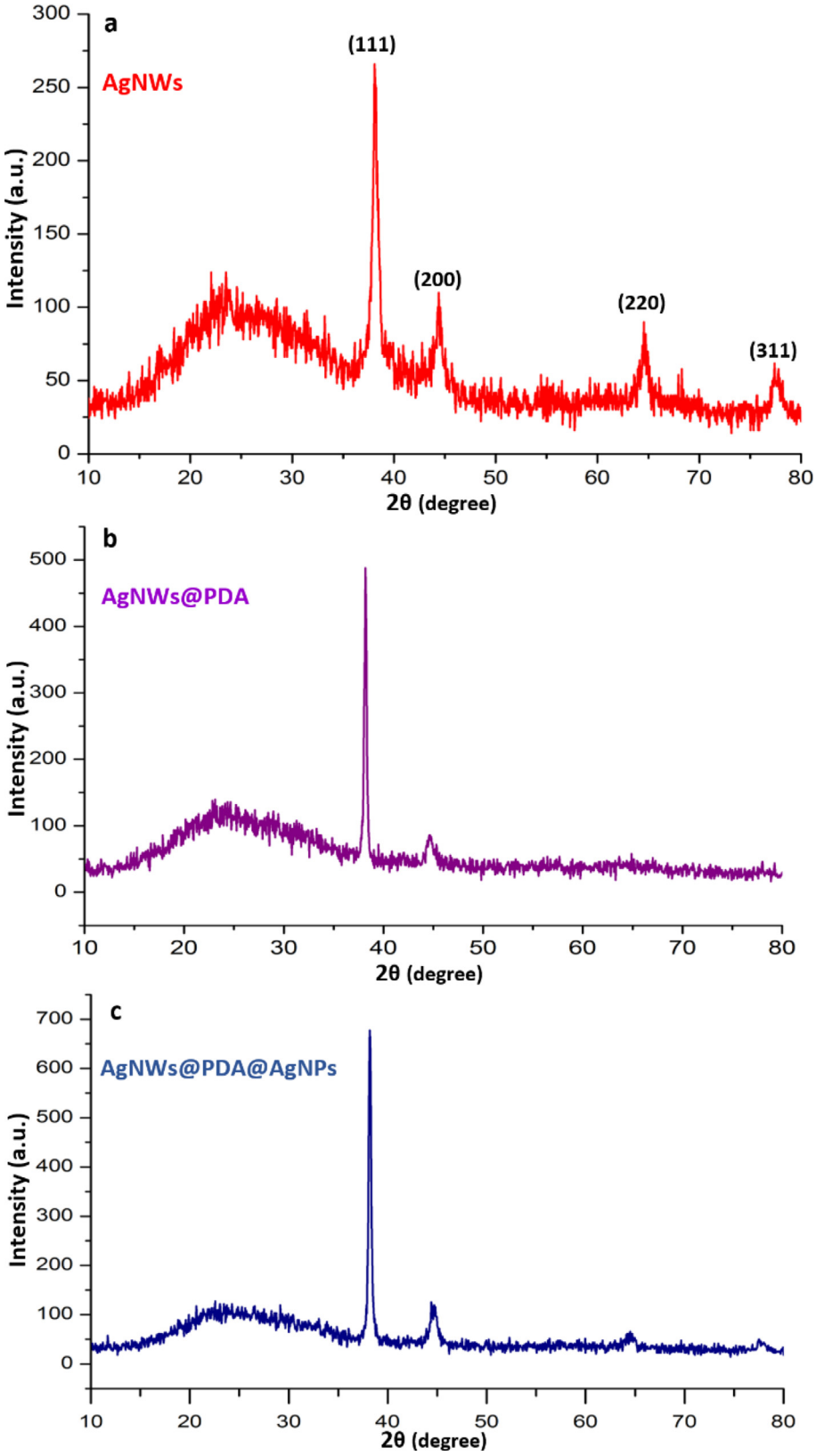

Fig. 3. X-ray diffraction patterns of (a) AgNWs, (b) AgNWs@PDA and (c) AgNWs@PDA@AgNPs nanostructures.

2.2. Fabrication of PSi substrates

After cutting the silicon samples into 2 × 2 cm^2 sections, the silicon (Si) substrate was washed in C_2H_5OH to remove dust and impurities. Then, it was etched in 10% diluted HF acid for 10 minutes to remove the SiO_2 coating. The silicon samples were placed in a plastic container filled with methanol to ensure that the Si surface was not oxidised during the reformation process.

PSi is made by an electrochemical etching technique. The experimental setup includes a DC power supply, a digital ammeter to test the passing current, a Teflon cell with high resistance to HF to prevent chemical reactions and a rubber O-ring between the silicon sample and the piece that holds the HF to prevent leakage. Fig. 2 shows how two electrodes, anode (Si) and cathode (gold mesh), are configured. The current density was based on the applied voltage, including 10 mA/cm^2. The etching time and HF concentration remain the same at 10 minutes and 15% respectively. Both samples were rinsed in pentane to prevent the PSi film from being easily removed, and then ethanol was used to extract the residual HF and pentane from the film.

3. Results and discussion

3.1. XRD patterns of AgNWs, AgNWs@PDA and AgNWs@PDA@AgNPs nanostructures

Distinctive XRD patterns of AgNWs, AgNWs@PDA, and AgNWs@PDA@AgNPs nanostructures are shown in Fig. 3. All trends have four peaks with minor differences in peak position between samples. These peaks were noticed at (2θ degree) of 38.117°, 44.277°, 64.426° and 77.472° respectively and have been indexed to (hkl) values of (111), (200), (220) and (311) respectively. Miller indices values match up with face-centred cubic of Ag metal that agree with JCPDS Card No. 4-0783. The prepared AgNWs, AgNWs@PDA and AgNWs@PDA@AgNPs nanostructures via the EEW technique showed no oxidation during and after the process, showing that they maintained excellent crystalline nature and good purity. The XRD pattern's peak location is close to that of normal bulk silver.

3.2. FE-SEM and TEM image analyses for nanostructures

The AgNWs generally have a smooth surface as well as a straight and consistent shape as shown in Fig. 4a. As can be seen in Fig. 4b, the PDA layer adhered to the AgNWs surface successfully. TEM

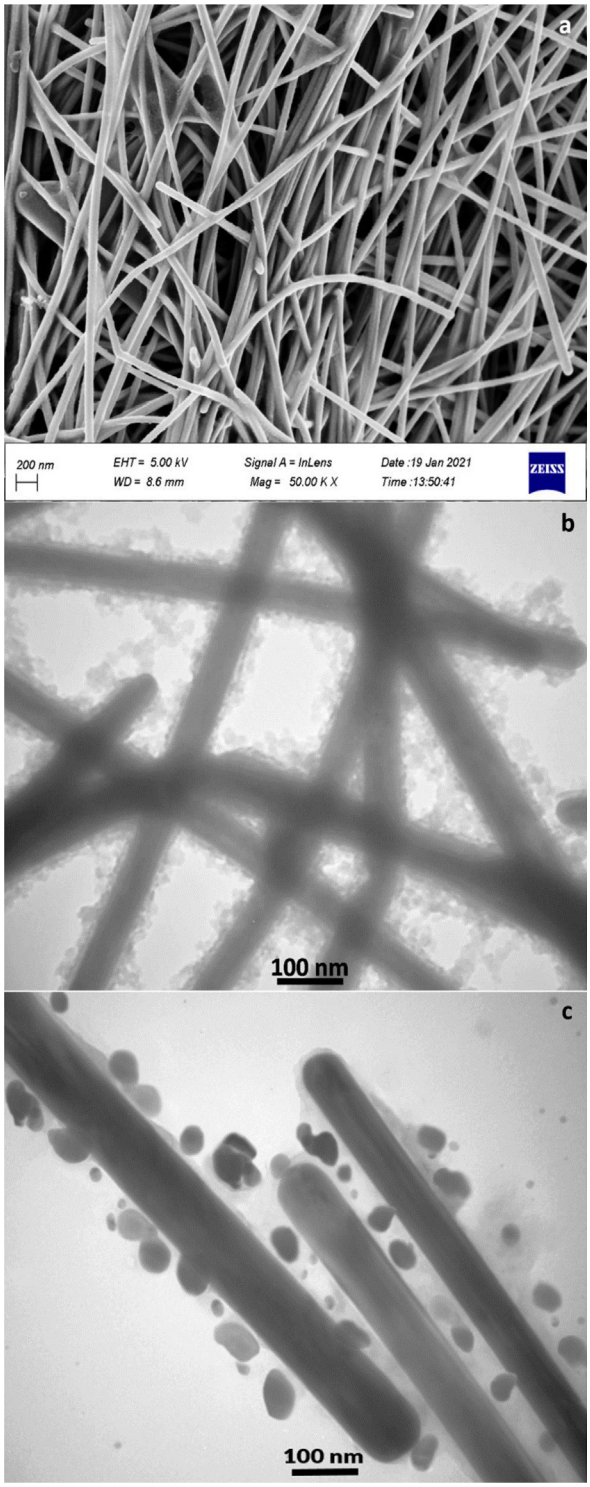

Fig. 4. FE-SEM image of (a) AgNWs nanostructures and TEM images of (b) AgNWs@PDA and (c) AgNWs@PDA@AgNPs nanostructures.

tests revealed the full covering of the AgNWs by the PDA layer to create the AgNWs@PDA nanostructure. The AgNWs were employed as a core and the PDA layer functioned as an amorphous shell. Fig. 4b shows how PDA molecules covered the surface of AgNWs

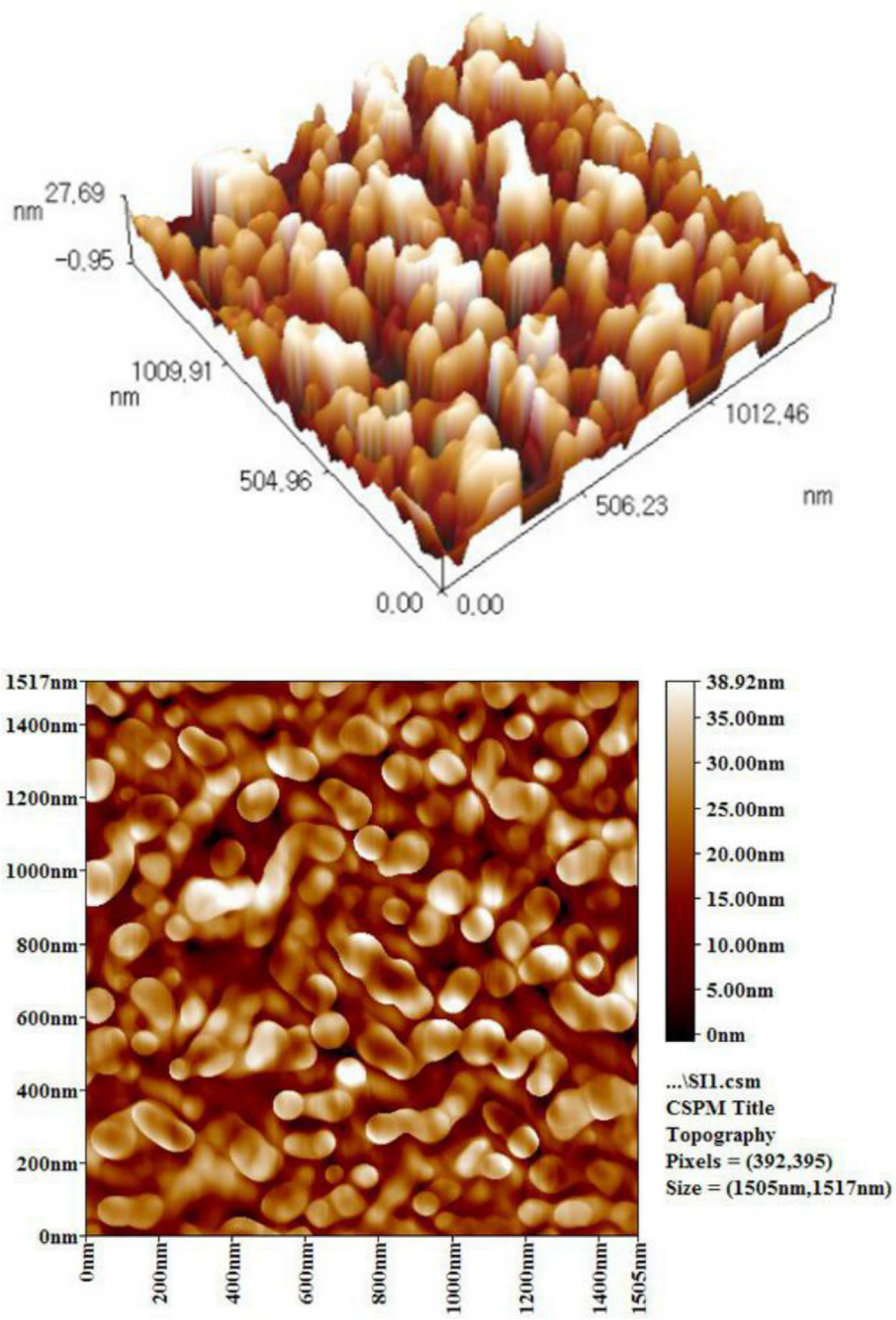

Fig. 5. 2D and 3D images of AFM analysis for PSi.

and self-polymerised them to form an assembled functional PDA layer. As shown in Fig. 4c, randomly distributed AgNPs decorated the surface of the AgNWs@PDA nanostructure and tightly clung to the surface to produce the AgNWs@PDA@AgNPs nanostructures. The PDA layer is employed as a spacer between the two metals, AgNWs and AgNPs, by acting as nanogaps. The number of explosions affects the density of AgNPs on the surface of AgNWs@PDA nanostructures. The distance between two nanostructures is several nanometres, which is the optimal spacing for effective hot spots to form due to electromagnetic interaction that is dependent on the PDA thickness [20,21].

3.3. Morphological properties of porous silicon (PSi)

The morphology of PSi layers samples was investigated using Atomic Force Microscopy (AFM).

The AFM studies are focused on the morphological properties at the nanometric scale of the PSi layers. The image in Fig. 5 shows that PSi with (100) n-type has a sponge-like structure after the etching time of 10 minutes. From the 3D image, the pore width and porosity increased with increasing etching time when HF concentration and current density remain constant. This happens because of the extra chemical dissolution of a PSi layer in HF.

The experimental determines the morphological aspects of the PSi surface, such as pore width, pore shape and silicon nano spacing between adjacent pores. Fig. 6 shows the AFM images of PSi-AgNWs and PSi-AgNWs@PDA@AgNPs substrates. In locations where AgNWs@PDA@AgNPs nanostructures improved, the density of the silver layer remained uniformly distributed throughout the silver nanoparticles on the surface. Many particles were tightly packed, allowing for "hot spots" to form and resulting in an improvement of the SERS signal. Since silicon pi features ordered pore channels vertically grown in silicon wafers, it stands out as an appealing material for the SERS substrate.

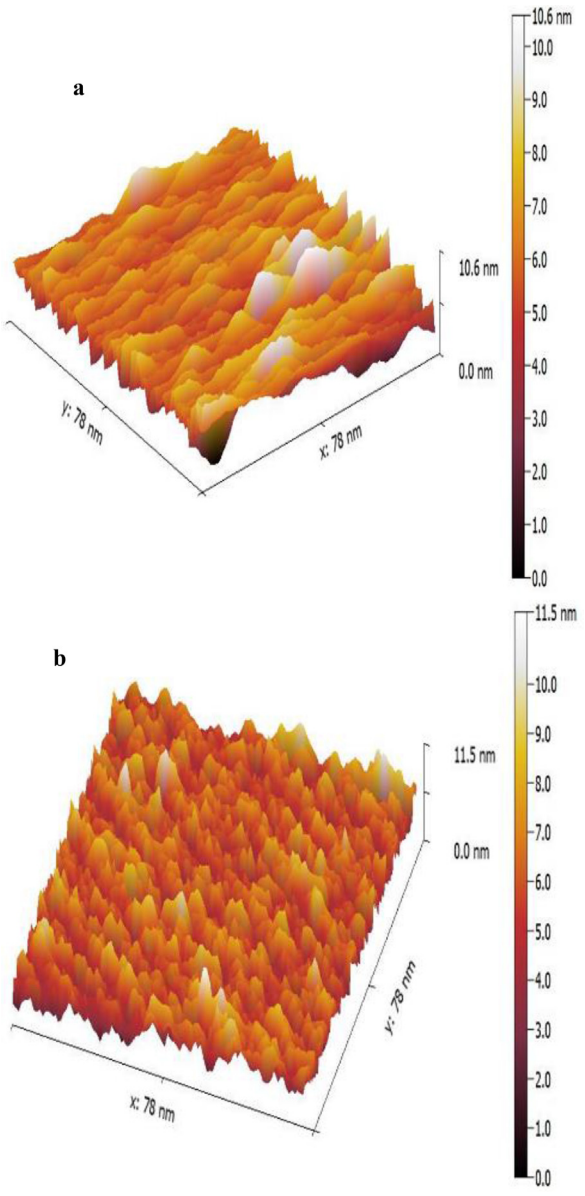

Fig. 6. 3D AFM images of the effectual substrates (a) PSi-AgNWs and (b) PSi-AgNWs@PDA@AgNPs.

3.4. UV-visible absorptance spectra

The UV–visible absorptances spectra of AgNWs at various concentrations (i.e., 4.5×10^{-4}, 3×10^{-4}, 2×10^{-4}, $1 \times 10^{-4}$and 0.5×10^{-4}) M in the presence and absence of Rh6G dye (1×10^{-6} M) is displayed in Fig. 7. Fig. 7a shows the AgNWs have two peaks of surface plasmon resonance (SPR). The first peak appears at 351 nm due to AgNWs' longitudinal Plasmon resonance absorptance. The second occurs at 375 nm due to AgNWs' transverse plasmon resonance absorptance [22]. With rising AgNWs concentration, the intensity of these peaks increases. The Rh6G dye molecules, on the other hand, have an absorptance peak at 524 nm as shown in Fig. 7b. The intensity of this peak increases as the AgNWs concentration rises. In an example of this behaviour, plasmonic metal nanostructures have demonstrated the capability to improve optical signals. The improved absorptance is based on the excitation of localised surface plasmons, which results in enhanced EM fields. As a result, molecules located within this enhanced field placed on the nanostructures will be stimulated more frequently due to the enhanced EM field of the incident light on the effectual substrate, resulting in improved absorptance [23,24].

In the absorptance spectrum of AgNWs, two distinct SPR peaks were observed at about 351 nm and 373 nm as shown in Fig. 8. When all AgNWs were coated with a PDA layer via self-polymerisation, the peaks almost vanished as displayed in the absorptance spectrum of AgNWs@PDA in Fig. 8a. The absorptance peak of AgNWs@PDA@AgNPs was seen at 400 nm. The AgNPs decorated AgNWs@PDA nanostructures with nano-spacer between AgNWs and AgNPs as surface Plasmon polariton (SPP) were used to create AgNWs@PDA@AgNPs nanostructures. The EM field significantly improved due to the coupling of LSP-SPP and LSP-LSP. When nanostructures were combined with RH6G dye, their absorptance peaks widened. The Rh6G dye molecules have an absorptance peak at 524 nm as shown in Fig. 8b. The intensity of this

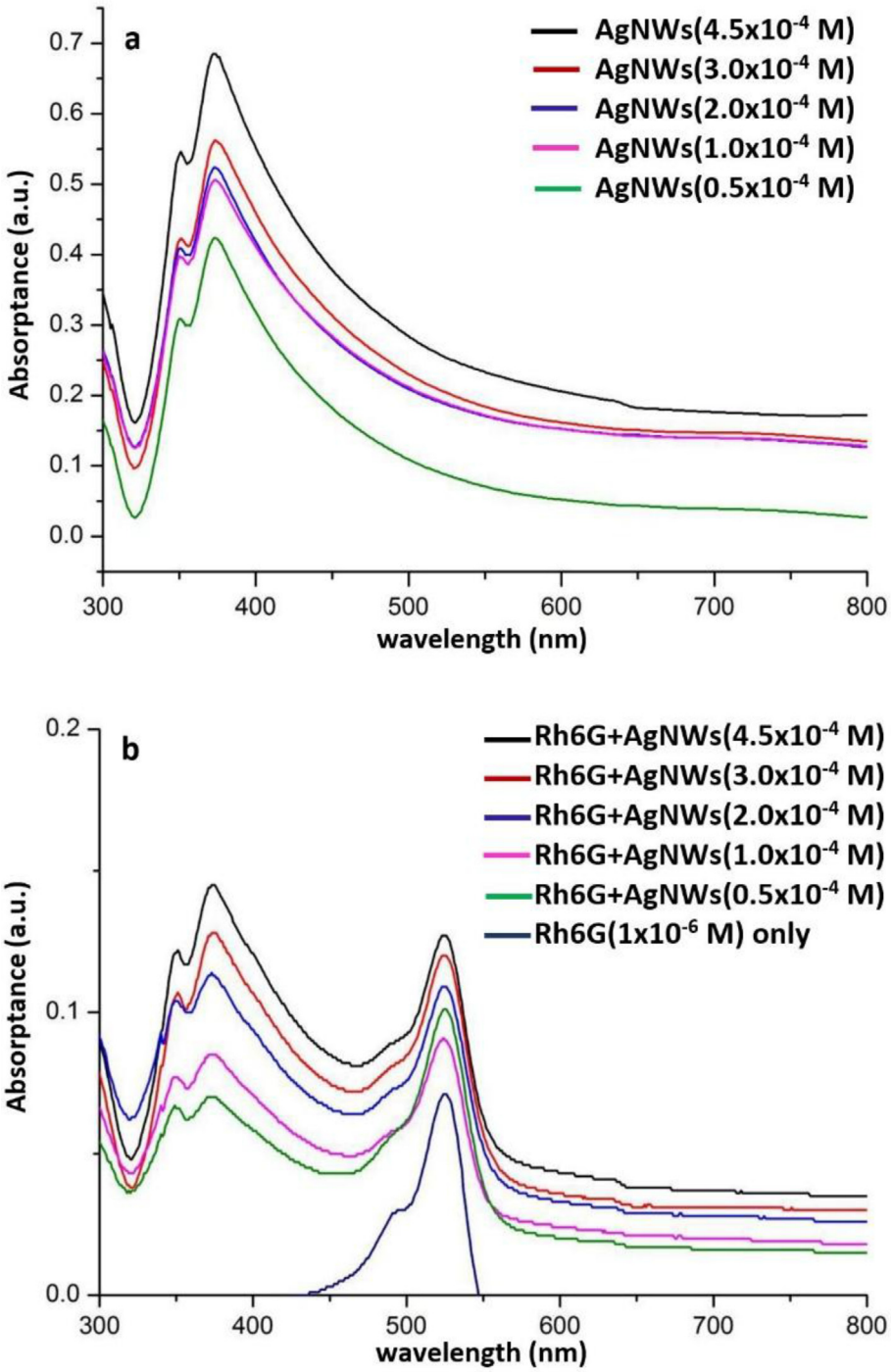

Fig. 7. The UV–visible absorptance spectra of different AgNWs concentrations (a) in the absence of Rh6G dye (b) in the presence of Rh6G dye (1×10^{-6} M).

peak rises when mixed with AgNWs and AgNWs@PDA@AgNPs. Because the SPR of metal nanostructures are highly sensitised to the dielectric environment between two metals, the SPR absorptance peaks of AgNWs@PDA@AgNPs nanostructures were enhanced more than those of the AgNW nanostructure [25].

3.5. Raman spectra of Rh6G dye

The Rh6G dye was used as probe molecules to prove the ability of the deigned substrates PSi-AgNWs and PSi-AgNWs@PDA@AgNPs to enhance SERS signals and test their ultra-sensitivity. Fig. 9a for PSi-AgNWs and Fig. 9b for PSi-AgNWs@PDA@AgNPs show the

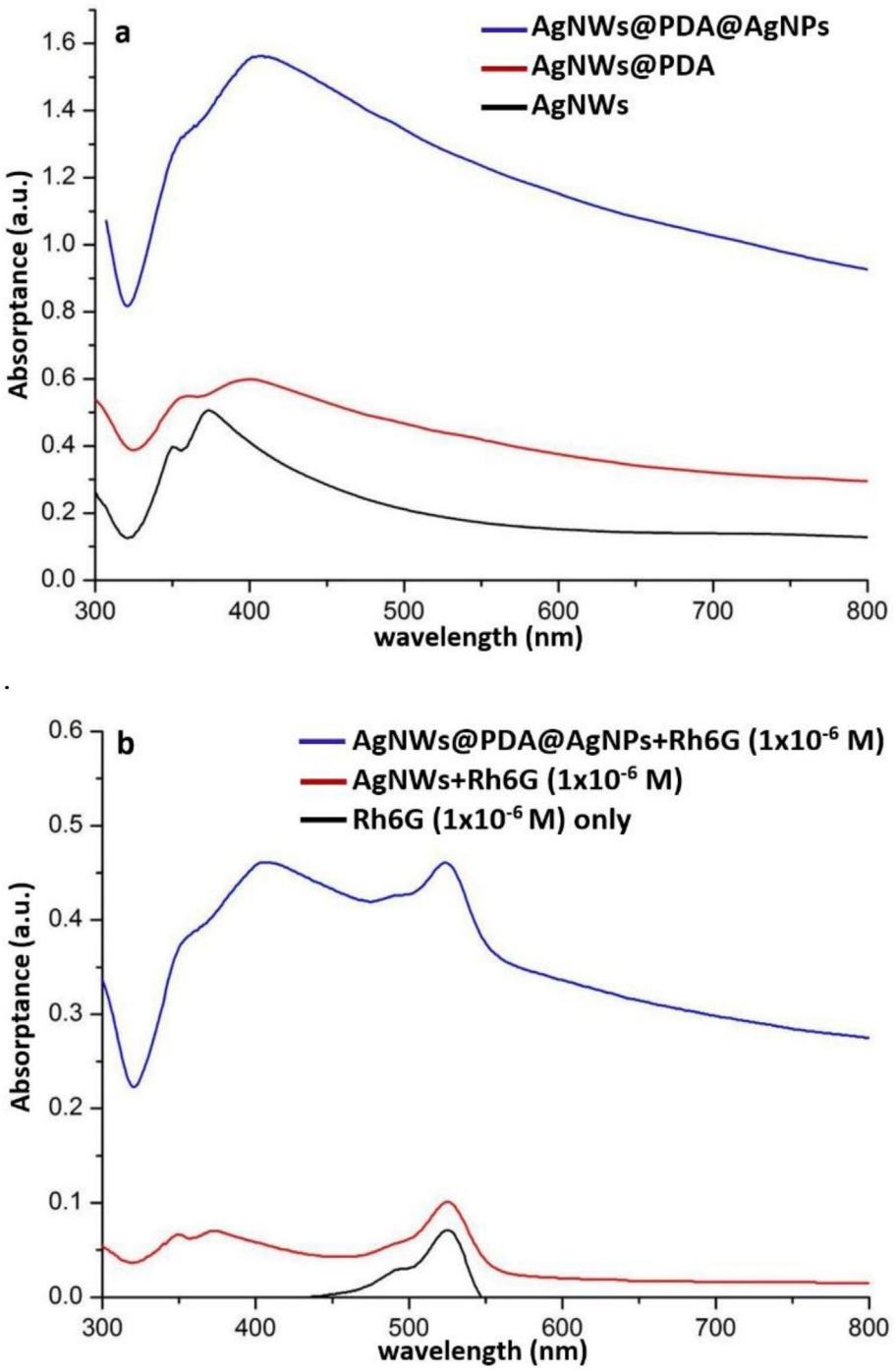

Fig. 8. The UV–visible absorptance spectra of AgNWs (0.5 × 10^{-6} M) and AgNWs@PDA@AgNPs nanostructures (a) without Rh6G dye (b) with (1 × 10^{-6} M).

Rh6G molecules spectra with a concentration of 1 × 10^{-1} M pure deposited on the glass substrate. It also illustrates the Rh6G molecules spectra at different concentrations (i.e., from 1 × 10^{-6} to 1 × 10^{-14} M) deposited on the PSi-AgNWs and PSi-AgNWs@PDA@AgNPs effectual substrates. Nanostructures were deposited and desiccated onto slides of porous silicon and then onto the Rh6G dye in a different concentration above the nanostructure. All samples have shown SERS activity and distinctive peaks after excitation with a 532 nm wavelength laser source and power of 4.5 mW. The sites of peaks at wavenumbers (i.e., 611, 776, 1187, 1315, 1361, 1510, 1575 and 1651 cm^{-1}) correspond respectively to the modes (C–C–C ring in-plane vibration), (C–H out of –plane bend), (C–H in-plane bend), (N–H in-plane bend),

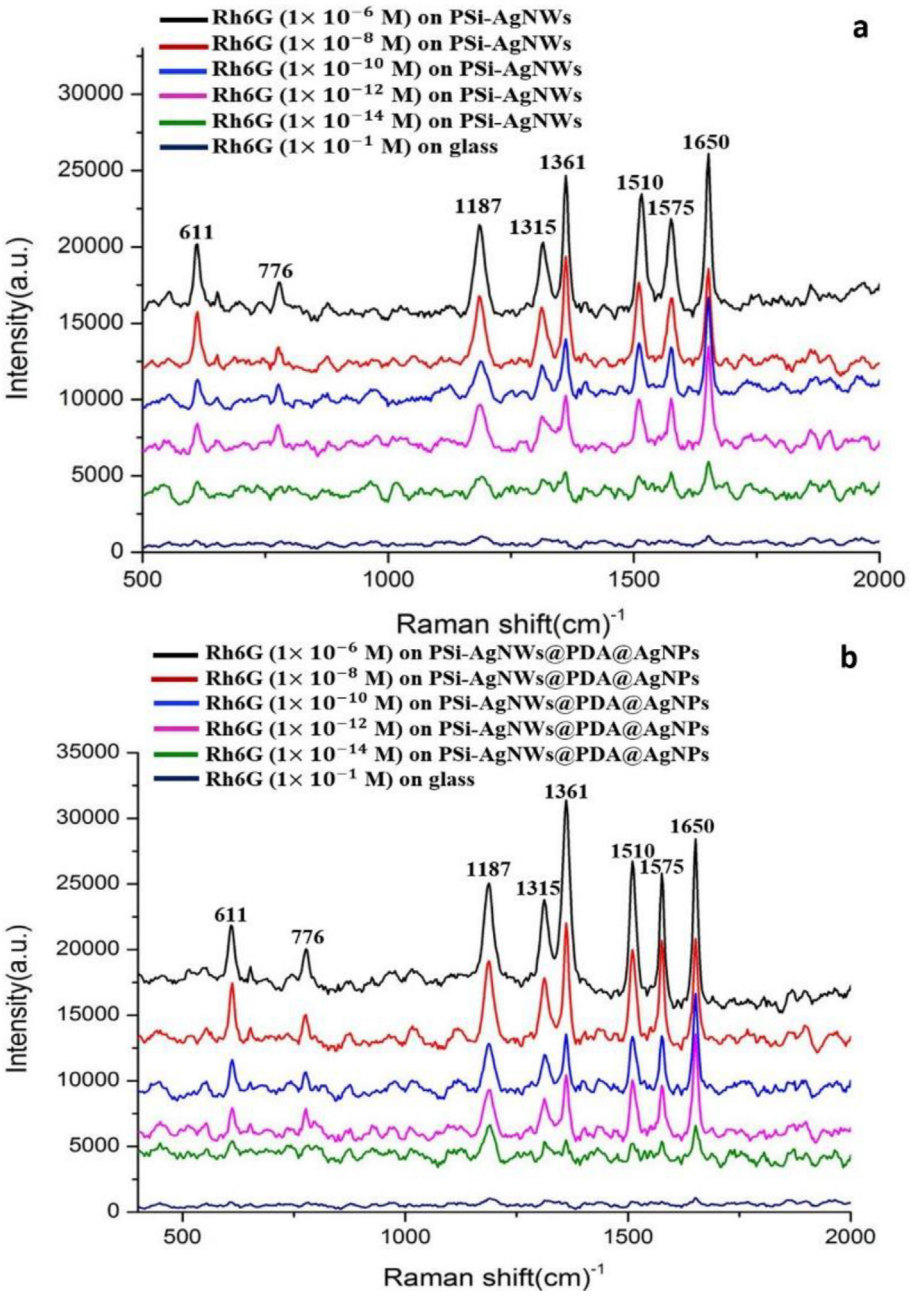

Fig. 9. Raman spectra of Rh6G dye from (1 × 10^{-6} M) to (1 × 10^{-14} M) on the (a) PSi-AgNWs substrate and (b) PSi-AgNWs@PDA@AgNPs substrate.

(C−C stretching), (C−C stretching), (N−H in-plane bend) and (C−C stretching). Raman shift in spectral ranged from 400 cm^{-1} to 2000 cm^{-1} with a detection limit of 1 × 10^{-14} M. It was discovered that the peak intensity of Raman signals decreased as concentration decreased, showcasing a linear relationship between the peak intensity of Raman signals and Rh6G dye concentration.

Fig. 10 shows SERS spectra of Rh6G molecules at 1 × 10^{-6} M for two deigned effectual substrates. The PSi-AgNWs@PDA@AgNPs effectual substrates were designed with an abundance of "hot spots," which are gaps or nano-spacers between two metals (e.g., AgNWs and AgNPs) that synergistically subscribe to the powerful SERS action. Furthermore, in AgNWs@PDA@AgNPs nanostructures, such small gaps between adjacent AgNPs and nano-spacer between AgNWs and AgNPs helped achieve an excellent SERS signal. The wavenumber peak of 1650 cm^{-1} was used to compute the enhancement factors (EFs) of the SERS signal of Rh6G dye on the PSi-AgNWs and PSi-AgNWs@PDA@AgNPs

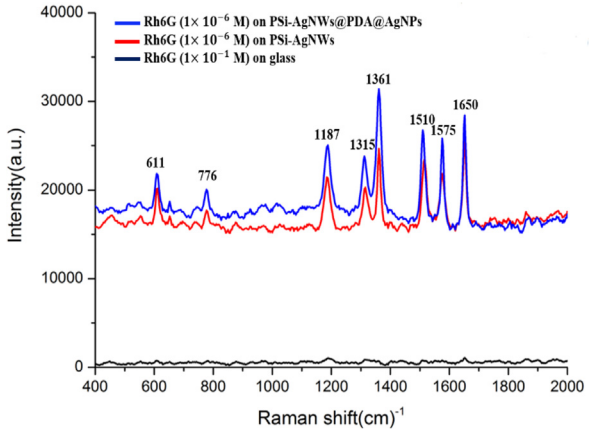

Fig. 10. Raman spectra of Rh6G dye (1 × 10^{-1} M) on glass substrate and Rh6G dye (1 × 10^{-6} M) on the PSi-AgNWs and PSi-AgNWs@PDA@AgNPs substrates.

substrates, and the following equation was utilized to compute the SERS EFs [18].

$$\mathbf{EF} = \frac{\mathbf{I_{SERS}}}{\mathbf{I_{bulk}}} \times \frac{\mathbf{N_{bulk}}}{N_{SERS}} \quad (1)$$

I_{SERS} is the Raman strength of the molecule with nanostructures, I_{bulk} is the Raman intensity of the molecule without nanostructures, N_{bulk} is the number of Rh6 G (1 × 10^{-6} M) molecules without nanostructures, and N_{SERS} is the number of Rh6G (1 × 10^{-6} M) molecules with nanostructures. As a result, the SERS EFs of Rh6G (1 × 10^{-6} M) reached (26.3 × 10^{-6}) and (28.7 × 10^{-5}) at the wavenumber peak 1650 cm^{-1} for the effectual substrates PSi-AgNWs and PSi-AgNWs@PDA@AgNPs respectively. The coupling between the localised surface plasmon (LSP) of the AgNWs and the many hot spots of the AgNWs@PDA@AgNPs nanostructures created via the AgNPs decoration on the surfaces of the AgNWs@PDA nanostructures produced a strong stimulation of the SERS signal by improving the EM field at hot spots.

4. Conclusion

Effectual substrates for SERS created using nanostructures-coated porous silicon are a wide topic of study. The analyte Rh6G was detected at a minimum concentration of 10^{-14} M, a limit like those of the best SERS-effectual substrates mentioned in published literature. Given the ease with which porous silicon can be made and covered with plasmonic nanostructures, it is reasonable to believe that SERS-effectual substrates with such characteristics can play a significant role in signal enhancement for SERS technique in analytical chemistry, materials science, pharmaceutics, medicine, and other fields. Two types of plasmonic associated with the nanostructure that contained of Ag nanowires coated with PDA layer and decorated with Ag nanoparticles (AgNWs@PDA@AgNPs), LSP-SPP and LSP-LSP, are formed by regulating the synergistic effect between two plasmonic metals, AgNWs and AgNPs, and the nano-layer separating them along the longitudinal axis of AgNWs. The AgNWs@PDA@AgNPs nanostructures have a considerable number of hot spots, therefore increasing the ultra-sensitivity of the SERS technique. By using this manufacturing technique, it is possible to create a wide range of effectual substrates and achieve a sensitive, reliable detection in biological and chemical fields.

References

[1] W. Wei, Y. Du, L. Zhang, Y. Yang, Y. Gao, Improving SERS hot spots for on-site pesticide detection by combining silver nanoparticles with nanowires, J. Mater. Chem. C 6 (2018) 8793–8803, https://doi.org/10.1039/c8tc01741g.
[2] E.B. Kaganovich, I.M. Krischenko, S.A. Kravchenko, E.G. Manoilov, B.O. Golichenko, A.F. Kolomys, V.V. Strel'chuk, SERS spectroscopy of nanocomposite porous films containing silver nanoparticles, Opt. Spectrosc. 118 (2015) 294–299, https://doi.org/10.1134/s0030400x1502007.
[3] R. Pilot, R. Signorini, C. Durante, L. Orian, M. Bhamidipati, L. Fabris, A review on surface-enhanced Raman scattering, Biosensors 9 (2019) 57, https://doi.org/10.3390/bios9020057.
[4] Z. Li, S. Jiang, Y. Huo, T. Ning, A. Liu, C. Zhang, Y. He, M. Wang, C. Li, B. Man, 3D silver nanoparticles with multilayer graphene oxide as a spacer for surface enhanced Raman spectroscopy analysis, Nanoscale 10 (2018) 5897–5905, https://doi.org/10.1039/c7nr09276h.
[5] X. Li, J. Li, X. Zhou, Y. Ma, Z. Zheng, X. Duan, Y. Qu, Silver nanoparticles protected by monolayer graphene as a stabilized substrate for surface enhanced Raman spectroscopy, Carbon 66 (2014) 713–719, https://doi.org/10.1016/j.carbon.2013.09.076.
[6] M. Zhang, H. Sun, X. Chen, J. Yang, L. Shi, T. Chen, Z. Bao, J. Leu, Y. Wu, Highly efficient photo-induced enhanced Raman spectroscopy (PIERS) from plasmonic nanoparticles decorated 3D semiconductor arrays for ultrasensitive, portable and recyclable detection of organic pollutants, ACS Sens. 4 (2019) 1670–1681, https://doi.org/10.1021/acssensors.9b00562.
[7] S. Rani, A.K. Shukla, Investigation of silver decorated silicon nanowires as ultrasensitive and cost-effective surface-enhanced Raman substrate, Thin Solid Films 723 (2021) 138595, https://doi.org/10.1016/j.tsf.2021.138595. .
[8] E.C. Le Ru, P.G. Etchegoin, Sub-wavelength localization of hot-spots in SERS, Chem. Phys. Lett. 396 (2004) 393–397, https://doi.org/10.1016/j.cplett. 2004.08.065.
[9] A.M. Alwan, L.A. Wali, A.A. Yousif, Optimization of AgNPs/mesoPS active substrates for ultra–low molecule detection process, Silicon 10 (2018) 2241–2251, https://doi.org/10.1007/s12633-018-9758-7.
[10] H. Guo, Z. Zhang, B. Xing, A. Mukherjee, C. Musante, J.C. White, L. He, Analysis of silver nanoparticles in antimicrobial products using surface-enhanced Raman spectroscopy (SERS), Environ. Sci. Technol. 49 (2015) 4317–4324, https://doi.org/10.1021/acs.est.5b00370.
[11] C. Wang, B. Liu, X. Dou, Silver nanotriangles-loaded filter paper for ultrasensitive SERS detection application benefited by interspacing of sharp edges, Sens. Actuator B Chem. 231 (2016) 357–364, https://doi.org/10.1016/j.snb.2016.03.030.

[12] H. Lee, S.M. Dellatore, W.M. Miller, P.B. Messersmith, Mussel-Inspired surface chemistry for multifunctional coatings, Science 318 (2007) 426–430, https://doi.org/10.1126/science.1147241.
[13] F. Hao, P. Nordlander, Plasmonic coupling between a metallic nanosphere and a thin metallic wire, Appl. Phys. Lett. 89 (2006) 103101, https://doi.org/10.1063/1.2345352.
[14] A.M. Alwan, I.A. Naseef, A.B. Dheyab, Well controlling of plasmonic features of gold nanoparticles on macro porous silicon substrate by HF acid concentration, Plasmonics 13 (2018) 2037–2045, https://doi.org/10.1007/s11468-018-0720-8.
[15] V. Mulloni, L. Pavesi, Porous silicon microcavities as optical chemical sensors, Appl. Phys. Lett. 76 (2000) 2523–2525, https://doi.org/10.1063/1.126396.
[16] Y. Liu, K. Ai, L. Lu, Polydopamine and its derivative materials: synthesis and promising applications in energy, environmental, and biomedical fields, Chem. Rev. 114 (2014) 5057–5115, https://doi.org/10.1021/cr400407a.
[17] J. Zhou, B. Duan, Z. Fang, J. Song, C. Wang, P.B. Messersmith, H. Duan, Interfacial assembly of mussel-inspired Au@Ag@ polydopamine core-shell nanoparticles for recyclable nanocatalysts, Adv. Mater. 26 (2013) 701–705, https://doi.org/10.1002/adma. 201303032.
[18] F.G. Hamzah, H.R. Mahmood, Signature of plasmonic nanostructures synthesised by electrical exploding wire technique on surface-enhanced Raman scattering, Iraqi J. Sci. 62 (2021) 167–179, https://doi.org/10.24996/ijs.2021.62.1.16.
[19] T.K. Al-Kafaji, H.R. Humud, Synthesis of Au–Ag–Cu trimetallic alloy nanoparticles prepared by electrical exploding wire technique in distilled water, Iraqi J. Phys. 16 (2018) 81–92, https://doi.org/10.30723/ijp.v16i39.106.
[20] F.H. Ho, Y.-H. Wu, M. Ujihara, T. Imae, A solution-based nano-plasmonic sensing technique by using gold nanorods, Analyst 137 (2012) 2545, https://doi.org/10.1039/c2an35101c.
[21] M. Piliarik, J. Homola, Z. Manikova, J. Ctyroky, Surface plasmon resonance sensor based on a single-mode polarization-maintaining optical fiber, Sens. Actuator B Chem. 90 (2003) 236–242, https://doi.org/10.1016/s0925-4005(03)00034-0.
[22] M.B. Gebeyehu, T.F. Chala, S.-Y. Chang, C.-M. Wu, J.-Y. Lee, Synthesis and highly effective purification of silver nanowires to enhance transmittance at low sheet resistance with simple polyol and scalable selective precipitation method, RSC Adv. 7 (2017) 16139–16148, https://doi.org/10.1039/c7ra00238f.
[23] S.F. Haddawi, H.R. Humud, S.M. Hamidi, Signature of plasmonic nanoparticles in multi-wavelength low power random lasing, Opt. Laser Technol 121 (2020) 105770–105771, https://doi.org/10.1016/j.optlastec.2019.105770.
[24] F.G. Hamzah, H.R. Humud, The Raspberry-like nanostructures (SiO2@AgNPs) fabricated by electrical exploding wire (EEW) technique for Raman scattering enhancement, AIP Conf. Proc. 2290 (2020), 0050033-1-11 https://doi.org/10.1063/5.0029719.
[25] Z. Zhang, T. Si, J. Liu, K. Han, G. Zhou, Controllable synthesis of AgNWs@PDA@AgNPs core–shell nanocobs based on a mussel-inspired polydopamine for highly sensitive SERS detection, RSC Adv. 8 (2018) 27349–27358, https://doi.org/10.1039/c8ra04936j.